Macromolecules

Article

pubs.acs.org/Macromolecules

Tough Supramolecular Hydrogel Based on Strong Hydrophobic Interactions in a Multiblock Segmented Copolymer

Marko Mihajlovic,[†,‡] Mariapaola Staropoli,[∥] Marie-Sousai Appavou,[⊥] Hans M. Wyss,[‡,§] Wim Pyckhout-Hintzen,[∥] and Rint P. Sijbesma*[,†,‡]

[†]Laboratory of Macromolecular and Organic Chemistry, Department of Chemical Engineering and Chemistry, [‡]Institute for Complex Molecular Systems, and [§]Department of Mechanical Engineering, Eindhoven University of Technology, P.O. Box 513, 5600 MB Eindhoven, The Netherlands

[∥]JCNS-1 and ICS-1, Forschungszentrum Jülich GmbH, Leo-Brandt-Straße, 52425 Jülich, Germany

[⊥]Jülich Centre for Neutron Science (JCNS) at MLZ, 85747 Garching, Germany

Supporting Information

ABSTRACT: We report the preparation and structural and mechanical characterization of a tough supramolecular hydrogel, based exclusively on hydrophobic association. The system consists of a multiblock, segmented copolymer of hydrophilic poly(ethylene glycol) (PEG) and hydrophobic dimer fatty acid (DFA) building blocks. A series of copolymers containing 2K, 4K, and 8K PEG were prepared. Upon swelling in water, a network is formed by self-assembly of hydrophobic DFA units in micellar domains, which act as stable physical cross-link points. The resulting hydrogels are noneroding and contain 75−92 wt % of water at swelling equilibrium. Small-angle neutron scattering (SANS) measurements showed that the aggregation number of micelles ranges from 2×10^2 to 6×10^2 DFA units, increasing with PEG molecular weight. Mechanical characterization indicated that the hydrogel containing PEG 2000 is mechanically very stable and tough, possessing a tensile toughness of 4.12 MJ/m^3. The high toughness, processability, and ease of preparation make these hydrogels very attractive for applications where mechanical stability and load bearing features of soft materials are required.

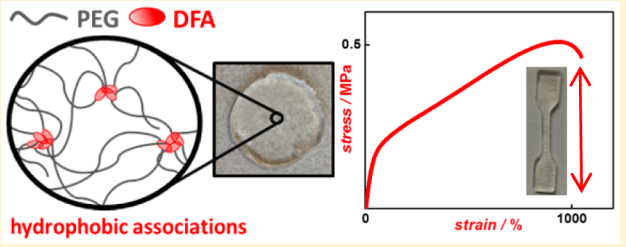

INTRODUCTION

Hydrogels are three-dimensional networks of hydrophilic polymers, able to absorb and retain large amounts of water, which makes them a very attractive class of materials for biomedical applications. Hydrogels are often biocompatible, primarily because of their hydrophilic character, high water content, and permeability similar to those of natural tissues. In the past decades, interest in hydrogels as drug delivery platforms, artificial implants, and scaffolds in tissue engineering has increased strongly.[1−6] However, most of the traditional synthetic hydrogels are brittle and possess poor mechanical properties.[7,8] These disadvantages can severely limit their application as very often they are required to have high toughness and load bearing features. Therefore, designing synthetic hydrogels with remarkable mechanical properties is an important task.

In order to improve mechanical properties of these soft materials, efficient energy dissipation mechanisms must be available at the molecular level because these increase resistance to crack propagation and lead to high toughness.[9,10] During the past few decades, many hydrogels with excellent mechanical properties have been developed, including hydrogels with homogeneous network structure,[11,12] topological,[13] nanocomposite,[14,15] double network,[16,17] and supramolecular hydrogels. Supramolecular hydrogels, also known as "reversible hydrogels", feature secondary interactions, such as H bonding,[18] ionic,[19] and hydrophobic interactions.[20] Because secondary interactions provide intrinsic mechanisms for energy dissipation, there is a large potential for designing high-toughness supramolecular hydrogels. Furthermore, being reversible, such materials can be handled and processed quite easily, which makes this type of hydrogel very attractive for use on a large scale.

Hydrophobic interactions have been extensively used in associative thickeners, such as hydrophobically ethoxylated urethanes (HEURs).[21,22] In these amphiphilic macromolecules, hydrophobic parts are able to self-assemble in flower-like micelles in aqueous solutions, bridging hydrophilic chains. This leads to increased viscosity due to the formation of a temporary physical network structure.[23,24] Based on the rheology of HEURs, introduction of hydrophobic interactions in hydrogel systems is expected to create reversible cross-links, which give gels the capability to flow and provide a mechanism to efficiently dissipate energy, increasing fracture toughness.[25,26] Okay and co-workers show that reversible hydrophobic

Received: February 13, 2017
Revised: March 23, 2017
Published: April 5, 2017

DOI: 10.1021/acs.macromol.7b00319
Macromolecules 2017, 50, 3333−3346

interactions in polyacrylamide hydrogels indeed contribute to improved mechanical properties.[10,20,27]

In analogy to thermoplastic elastomers, multiblock, segmented copolymers with hydrophobic segments are expected to endow gels with higher elasticity and reduced creep. Indeed, in hydrogels based on the segmented copolymer between hydrophilic PEG and 2-ureido-4[1*H*]-pyrimidinone (UPy) hydrogen-bonding units, developed by Meijer and co-workers, it was shown that due to microphase-separated network, hydrogels exhibited high strength and resilience when deformed.[28] In our group, an injectable, elastic hydrogel was developed, based on the segmented copolymer containing PEG and bisurea segments.[29]

In light of designing hydrogels that are easy to prepare and process, while maintaining high toughness, we were inspired by the above-mentioned studies and wanted to design a supramolecular hydrogel that would include multiblock, segmented polymer architecture and strong hydrophobic interactions. We anticipated that by bringing together these two concepts in one system, we could produce a single-network, high-toughness supramolecular hydrogel based solely on hydrophobic interactions. With this in mind, we chose our building blocks: poly(ethylene glycol) (PEG), a water-soluble polymer, widely used in many hydrogel preparations because of its nontoxicity and biocompatibility,[30−33] and dimer fatty acid (DFA).[34] DFA is a fully hydrogenated C36 hydrophobe, a dimer of stearic acid. It has a well-defined molecular weight but it is a mixture of different isomers, which prevents crystallization in applications in polymers.[35] The novelty of our hydrogels is precisely the use of DFA, and we chose it because of its large size, which we anticipated would form stable and robust physical cross-links, leading to improved mechanical properties. To the best of our knowledge, so far such a large hydrophobe has not been used in hydrogel formulations.

In the present work we report on a simple and fast method to prepare hydrophobically associated supramolecular hydrogels, starting from inexpensive and readily available building blocks. Segmented copolymers were prepared by polycondensation reaction between PEG and DFA (or its diisocyanate derivative, DDI) without adding any surfactant molecules and/or chemical cross-linking agents. Hydrogels made by this method are expected to display high mechanical strength, toughness, and stability due to the multiblock architecture of the polymer and strong hydrophobic aggregation between DFA units. We aimed to explore structural, viscoelastic, and mechanical features of these hydrogels and determine whether a high degree of toughness is achieved.

EXPERIMENTAL SECTION

Materials. Poly(ethylene glycol) (PEG) 4000 and 8000, dimerized fatty acid (DFA), and dibutyltin dilaurate (DBTDL) (95%) were all purchased from Sigma-Aldrich. Poly(ethylene glycol) (PEG) 2000 was obtained from Merck. Dimer fatty acid-based diisocyanate (DDI 1410, 92% pure) was kindly provided as a free sample by Cognis (now BASF). Tin(II) chloride anhydrous ($SnCl_2$) (99%) was purchased from Alfa Aesar. Bulk solvents were obtained from Biosolve BV Chemicals and used as received. All PEG compounds were dried by azeotropic distillation with toluene before use. Other chemicals were used without further purification.

Synthesis. *Segmented PEG-DFA-Based Copolymer.* In a 300 mL three-neck round-bottom flask flange reactor with a magnetically coupled anchor stirrer, PEG 2000 (30.00 g, 15 mmol) was melted at 150 °C, and the vacuum was applied for 20 min. When completely dry PEG was obtained, DFA (8.55 g, 15 mmol) and $SnCl_2$ (193 mg, 0.5 wt % of the total amount of monomers) were added to the reaction mixture, vacuum was reapplied, and a cold trap was set. The temperature was increased to 180 °C for 1 h. Finally, the temperature was increased to 200 °C, and the reaction mixture was stirred under reduced pressure (0.1−0.2 mbar) for 24−30 h (until the mixture became so viscous that no efficient stirring could be observed anymore). After that time, the vessel was slowly cooled down to room temperature at atmospheric pressure, and the reaction was quenched by adding approximately 100 mL of chloroform under stirring. The resulting chloroform solution was then precipitated into an excess amount of diethyl ether and centrifuged at 20 000 rpm for 10 min. The final product was isolated as a white powder, and it was dried under reduced pressure at room temperature overnight.

Segmented PEG-DDI-Based Copolymer. In a typical reaction, previously dried PEG 2000 (7.00 g, 3.5 mmol) was dissolved in 10 mL of chloroform in a 50 mL two-neck round bottom flask, and DBTDL (44 μL, 0.5 wt % with respect to the total amount of monomers) was added under argon flow. Next, DDI (2.26 g, 3.85 mmol) was dissolved in 3 mL of chloroform and added dropwise to the reaction mixture. The reaction mixture was stirred under argon, at reflux (75 °C) for 12 h, until significant increase in viscosity was observed. At this point, the reaction was stopped by cooling down the flask to room temperature and adding small amount of chloroform (10 mL). The resulting solution was precipitated in large amount of diethyl ether and centrifuged at 20 000 rpm for 10 min. The final product was dried under reduced pressure at room temperature overnight and appeared as white powder. The same procedure was employed for the synthesis of PEG 4000-DDI and PEG 8000-DDI segmented copolymers.

Gel Permeation Chromatography (GPC). GPC (PL-GPC 50 Plus) with integrated refractive index detector (Polymer Laboratories) was used to obtain molecular weights (MWs) of the synthesized segmented copolymers. The samples were prepared in dimethylformamide (DMF) with 10 mM LiBr at 5 mg/mL and filtered through PTFE syringe filters (from VWR) with average pore size of 0.2 μm. DMF with 10 mM LiBr was used as mobile phase at a flow rate of 1.0 mL/min. GPC data reported for the MWs are relative to a calibration based on PEG standards (Polymer Source).

NMR Spectroscopy. ^{1}H NMR spectra of the samples were obtained by employing a Varian Mercury VX (400 MHz) spectrometer. Solutions were prepared in $CDCl_3$ (Cambridge Isotope Laboratories), and measurements were performed at room temperature. Chemical shifts are reported as δ in parts per million (ppm) and referenced to tetramethylsilane (at 0 ppm).

Fourier-Transformed Infrared Spectroscopy (FT-IR). FT-IR spectra were recorded at room temperature on a PerkinElmer Spectrum One spectrometer equipped with a universal attenuated total reflectance (ATR) sampling accessory. The samples were scanned in the range from 450 to 4000 cm^{-1} with a 8 scan per sample cycle and a resolution of 4 cm^{-1}.

Hydrogel Preparation. Polymer disks of 25 mm in diameter and 0.5 mm thickness were obtained by compression-molding. The powder-like material was melt-pressed at 95 °C at a pressure of 100 bar for 10 min using a stainless steel mold; within the mold the material was sandwiched between two pieces of Teflon sheets to prevent sticking. After cooling to room temperature, polymer disks were removed from the mold, and their weight was recorded prior to the subsequent swelling experiments. Hydrogels were then obtained after the above-mentioned disks were immersed in a large excess of water at ambient temperature for a minimum of 24 h.

Hydrogel Swelling, Determination of Equilibrium Water Content (EWC), and Stability Studies. Swelling properties and EWCs of the hydrogels were measured at room temperature using a gravimetric method. The discs were placed in distilled water at room temperature, and their weight gain was measured as a function of time. Each sample was weighed before soaking. At designated periods of time, they were taken out of the bath, gently blotted with filter paper to remove surface water, immediately weighed, and returned to the bath. The water content at different times can be calculated by the equation

DOI: 10.1021/acs.macromol.7b00319
Macromolecules 2017, 50, 3333−3346

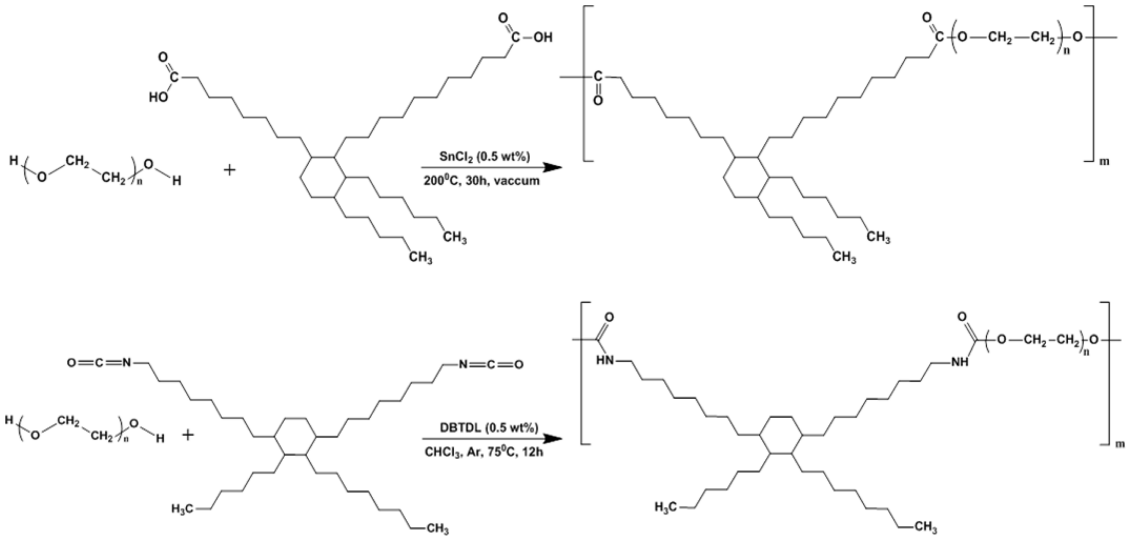

Figure 1. Synthetic procedures for the preparation of the segmented polyester (top) and polyurethanes (bottom), obtained via polymerization reactions.

$$W\ (\%) = \frac{m - m_0}{m} \times 100 \quad (1)$$

were m_0 and m are the weights of the dry sample and hydrogel at the time of measurement, respectively. W (%) is the water content, while EWC (%) indicates the water content when the equilibrium is reached. The stability of the hydrogels at swelling equilibrium was investigated by the same method. Hydrogel was stirred in distilled water at room temperature, and the weights were taken at defined times for the next 50 days. Fresh water was replaced each time the measurement took place.

Small-Angle Neutron Scattering (SANS). SANS measurements were performed at the KWS-2 diffractometer at MLZ, Munich, Germany. Data were recorded at different sample-to-detector distances (D = 1.4, 2, 8, and 20 m) and corresponding collimation lengths covering the scattering vector (q) range between 0.002 and 0.3 Å^{-1}. The scattering vector is given by $q = (4\pi/\lambda)\ \sin(\theta/2)$, where θ is the scattering angle. The employed neutron wavelength was λ = 5 Å with relative width 20%, and the scattering intensity was detected by means of a two-dimensional detector consisting of 128 × 128 channels, with the size of each channel 6 mm × 6 mm. Data were corrected for detector sensitivity, transmission, background, and empty cell scattering and were radially averaged. The scattering was calibrated for absolute intensity using a 1.5 mm thick PMMA standard.

All samples were prepared in Hellma quartz cells with a 1 mm path length, and the measurements took place at room temperature. Dry, powder-like materials were dissolved in a small amount of acetone in the cells, and then the solvent was removed under vacuum at 40 °C overnight. The aforementioned dry films were swollen to hydrogel state with deuterium oxide (99.9 atom % D, Sigma-Aldrich) at the desired concentration. D_2O was chosen as solvent because its scattering length density (ρ_{D_2O} = 6.36 × 10^{10} cm^{-2}) strongly differs from that of PEG (ρ_{PEG} = 6.34 × 10^{9} cm^{-2}) and the segregating DFA moieties (ρ_{DFA} = 1.67 × 10^{9} cm^{-2}). Therefore, the scattering intensity from PEG under these conditions is nonzero. These PEG segments could have been matched or made "invisible" to neutrons if a mixture of about 16% D_2O/84% H_2O was taken as the solvent. However, this would have reduced at the same time the contrast to the DFA units by roughly a factor of 240 and increased the incoherent background by about 3, both conditions not recommendable for accurate experimenting. The cells were properly sealed to prevent any evaporation during the measurement.

Rheology. Viscoelastic properties of the hydrogels were studied by rheology. Oscillatory shear and stress relaxation measurements were determined by a stress-controlled rheometer (Anton Paar, Physica MCR501). The measuring device was equipped with plate−plate geometry (25 mm in diameter) and a temperature unit (Peltier hood accessory), which provides temperature control and prevents evaporation during the experiments. All measurements were conducted on hydrogel samples at 25 wt % concentration and at 25 °C unless otherwise noted. Dynamic measurements were performed over a frequency range of 0.1−100 rad/s using a shear strain of 0.1%, whereas in the stress relaxation experiments a step strain of 0.1% was applied, and the decay of stress in the viscoelastic material is monitored as a function of time. The temperature sweep experiment was done at a constant heating rate of 2 °C/min over a temperature range between 25 and 75 °C.

Tensile Testing. Mechanical properties were determined by tensile testing, in both uniaxial extension mode and cyclic testing mode. Tests were carried out with Zwick Z100 universal tensile tester with the load cell of 100 N at room temperature. For uniaxial extension tests, the crosshead speed was set at 5 mm/min, while for the cyclic tests at low strains, the speed was 0.5 mm/min. Dog-bone samples were cut from rectangular hydrogel films previously brought to swelling equilibrium. They were kept in water until the measurements took place. The sample size was 12.5 mm length, 2 mm width, and 1.5 mm thickness, as measured prior to testing. Sample grips were tightly fixed between the clamps to prevent eventual slippage during the loading. The measurements were performed on at least five samples, and the results were averaged. Standard deviations of all recorded parameters were less than 10%. From the stress−strain curve, tensile modulus, tensile strength, elongation at break, and toughness were determined. Tensile modulus was calculated as the slope of the linear portion of the curve (1−4%) by using the linear regression method. Tensile strength corresponds to the maximum stress absorbed by material, while elongation at break is relative to the maximum extension of the sample before failure. Tensile toughness was determined by integrating the area under the curve from the start of the test until fracture of the sample.

RESULTS AND DISCUSSION

Synthesis and Molecular Characterization. The one-step synthesis of the segmented copolyester based on PEG diol and DFA is schematically represented in Figure 1 (top), and the adopted synthetic methodology is a modification of a literature procedure for esterification of DFA with PEG, consisting of reacting DFA and PEG diol in stoichiometric ratio at 200 °C, under vacuum and in the presence of tin(II) chloride as a catalyst for 30 h.[36] The reaction is a typical polycondensation polymerization, in which ester bonds are

DOI: 10.1021/acs.macromol.7b00319
Macromolecules 2017, 50, 3333−3346

Table 1. Characteristics of the Segmented Copolymers

sample name	M_w (kg/mol)	M_n (kg/mol)	M_w/M_n	bond type	PEG MW	apolar unit
PE PEG2000	70	29	2.41	ester	2000	DFA
PU PEG2000	35.3	19	1.86	urethane	2000	DDI
PU PEG4000	48.2	33.3	1.45	urethane	4000	DDI
PU PEG8000	84.2	61.5	1.37	urethane	8000	DDI

formed between hydroxyl groups of PEG diol and carboxylic acid functionalities of DFA. In order to study how mechanical and viscoelastic properties of the resulting hydrogels are affected by the hydrophobic/hydrophilic balance, we varied the hydrophilicity by incorporating different molecular weights of PEG diol. PEG2000, PEG4000, and PEG8000 diols were reacted with DFA to give segmented copolymers. However, the literature procedure consistently gave low molecular weight polymers when PEG4000 and PEG8000 were used, most likely due to the lower concentration of functional groups in the reaction mixture. A successful alternative to segmented copolyester was the synthesis of the corresponding polyurethane. In this approach, DFA diisocyanate (DDI) was used, and the urethane bonds were formed via the addition reaction between isocyanate groups of DDI and hydroxyl groups of PEG diol[37] (Figure 1, bottom). Using this procedure with some modifications, three segmented polyurethanes were prepared, with PEG2000, PEG4000, and PEG8000, as summarized in Table 1.

We use the following nomenclature in order to distinguish the samples by their composition: P*X* PEG*Y*, where *X* is either E (ester) or U (urethane) and *Y* is the molecular weight of the PEG in g/mol. Four segmented copolymers containing alternating hydrophilic (PEG) and hydrophobic (DFA) segments were prepared on a multigram scale and characterized with GPC, IR, and ^{1}H NMR spectroscopy.

The molecular weights and molecular weight distributions were determined by GPC and are listed in Table 1. PE PEG2000 and PU PEG2000 have relatively broad distribution of molecular weights (2.4 and 1.86, respectively), which is expected for condensation polymerization reactions. In the materials with high molecular weight PEG, polydispersity is below 1.5, but lower molecular weight species, corresponding to oligomers, are present in the product (see Supporting Information, Figure S1).

Figure 2 displays FT-IR spectra of the reactants and resulting segmented copolymers. The characteristic peaks of the end −COOH group at 1708 cm^{-1} and the −OH group at 3400−3500 cm^{-1} present in the starting materials have completely disappeared in the spectrum of copolyester PE PEG2000, while a new absorption band appeared at 1735 cm^{-1}, due to the −C═O ester stretch vibration (Figure 2, left). Thus, IR showed that the reaction between COOH of DFA and OH of PEG2000 diol was successful, and it resulted in the formation of ester bonds.

Similarly, the formation of the urethane bonds was observed in the polymers synthesized from DFA diisocyanate. The spectra in Figure 2 (right) show the characteristic bands present in the reactants: stretch of the isocyanate group (−N═C═O) at 2260 cm^{-1} and a weak broad band of the end −OH groups of PEG diol at 3400−3500 cm^{-1}. In the product, bands of the urethane bond (−NH−CO-O−) appeared as a weak signal around 3350 cm^{-1}, attributed to the N−H stretch vibration and two characteristic signals at 1721 cm^{-1} (−C═O stretch) and N−H in-plane bending at 1532 cm^{-1}. The presence of these bands and the disappearance of the characteristic bands of the reactants confirmed the formation of urethane bonds in these segmented copolymers.

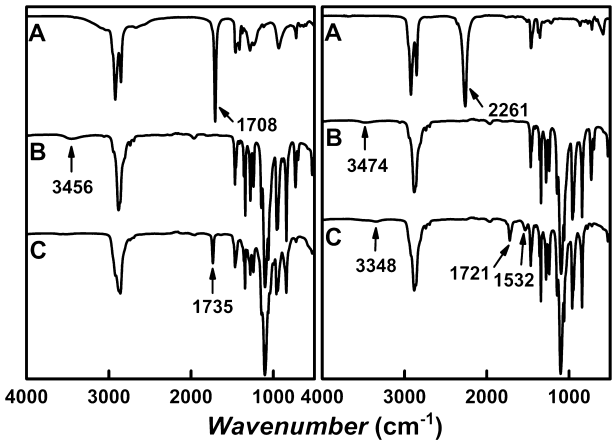

Figure 2. FT-IR spectra of (left) reactants DFA (A), PEG2000 diol (B), and segmented polyester PE PEG2000 (C); (right) reactants DDI (A), PEG2000 diol (B), and polyurethane PU PEG2000 (C).

Finally, the copolymers were also characterized by ^{1}H NMR spectroscopy with the spectra shown in Figure S2 (Supporting Information), with all signals in line with the proposed structures.

Swelling Behavior, EWC, and Stability of Hydrogels. Because of the hydrophilic nature of the PEG segments, PEG-DFA-based copolymers absorb water when soaked, giving rise to transparent hydrogels, which have mechanical integrity due to aggregation of the highly apolar DFA units, which phase separate and act as reversible cross-links in the network (Figure 3a).

Water absorption during soaking was measured gravimetrically and is plotted as a function of swelling time in Figure 3b. All samples were 0.5 mm thick disks with a diameter of 25 mm. The equilibrium amount of the absorbed water increased with PEG weight fraction from 75% for PE PEG2000 to 92.5% for PU PEG8000. All polymer samples showed similar swelling kinetics: 86−90% of the amount of water absorbed at equilibrium is taken up in the first 30 min upon soaking, and equilibrium was reached in less than 6 h for all samples.

The hydrogels are insoluble in water. The stability over longer periods of time was tested for PE PEG2000, mechanically the most stable material. A sample stored in water showed no weight loss over a time of 50 days (Figure 3c). The stability of the same polymer was also studied in a 10% (w/v) solution of sodium dodecyl sulfate (SDS). After 5 days, the hydrogel had completely dissolved. This indicates that surfactant molecules were able to significantly weaken the hydrophobic interactions, resulting in disruption of the network and solubilization of the hydrogel.[38]

Structural Characterization: SANS Analysis. Since segmented copolymers are able to form mechanically robust hydrogels, we propose a morphology for the micellar network

DOI: 10.1021/acs.macromol.7b00319
Macromolecules 2017, 50, 3333−3346

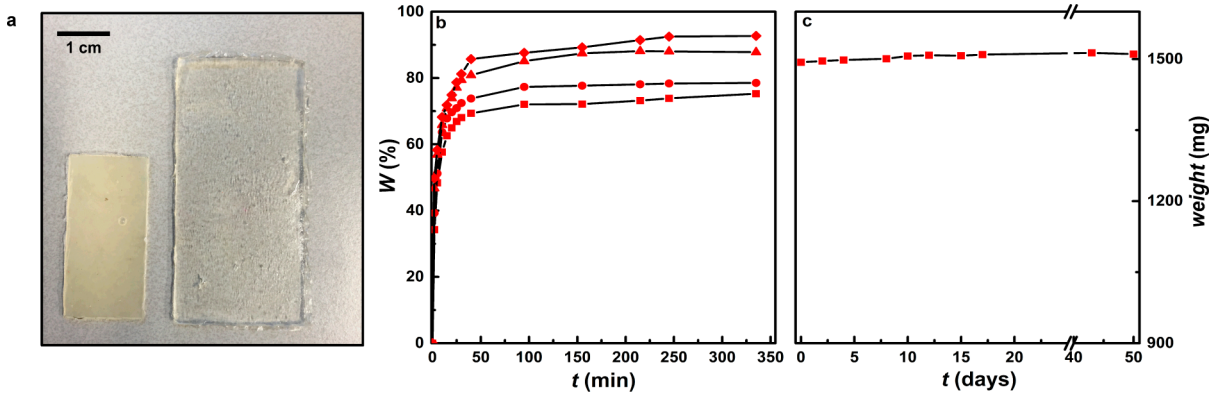

Figure 3. (a) Dry and equilibrium-swollen films of PE PEG2000; (b) swelling properties of the segmented copolymers and corresponding EWCs; (c) stability study of PE PEG2000, plotted as weight variation versus time; segmented copolymers are as follows: (■) PE PEG2000, (●) PU PEG2000, (▲) PU PEG4000, and (◆) PU PEG8000.

as illustrated in Figure 4, in which the network is formed via aggregation of hydrophobic (DFA) segments. These units

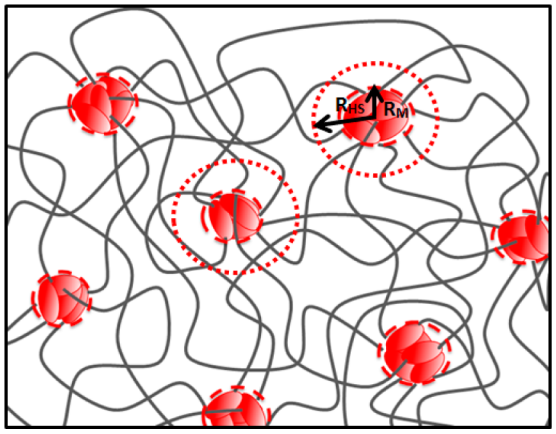

Figure 4. Physically cross-linked network of PEG-DFA hydrogels; DFA hydrophobic aggregates (in red) and PEG chains (in black). R_{HS} is equivalent hard sphere radius according to Percus−Yevick model; R_M is mean micellar radius.

microphase-separate from the hydrophilic PEG segments, driven by hydrophobic interactions. Considering that the volume fraction of DFA component in the copolymers is relatively low (6.7%, 12.7%, and 22.7% for PEG8000, PEG4000, and PEG2000 copolymers, respectively), and according to the theory of block copolymer self-assembly, we may safely assume the morphology of the DFA nanodomains to be spherical.[39−41] Then, they act as cross-link points that are bridged and surrounded by PEG chains, which results in the formation of a classical multifunctional network. In order to investigate in detail the microstructure and nanoscale morphology of the prepared hydrogels, SANS measurements were performed.

SANS data were recorded for four hydrogels (PE PEG2000, PU PEG2000, PU PEG4000, and PU PEG8000) at room temperature, at their equilibrium swelling state, as well as in a more concentrated regime. As we are interested in the size and spacing of the associating DFA domains, for reasons of accuracy data were recorded in pure D_2O only. These domains are diluted in the gel, consisting of PEG and D_2O which constitutes thus a three-component system. Absolute scattering intensities vs scattering vector q are shown in Figure 5a. Below, the data are first described qualitatively, followed by discussion in full detail.

All spectra exhibit similar intensity profiles, even at different concentrations, which suggests that all hydrogels have similar nanoscale structures. All profiles show the presence of a distinct peak at a characteristic q value varying between 0.03 and 0.09 $Å^{-1}$ as a function of the parameters of the gels. The position of the peak maximum q_{max} is indicative of a characteristic distance in real space and can be related to an average spacing between DFA nanodomains.[29,42,43] According to Bragg's law, the spacing D is given by $D = 2\pi/q_{max}$. Similar diffraction peaks have been observed in PEG-based hydrogels with high functionality cross-link points.[44] In the present hydrogels, DFA domains act as massive cross-link points with concentrated scattering length density and therefore show up as distinct scattering objects.

It is evident from Figure 5a that the position of the peak varies among the samples and depends on both concentration and composition. Upon dilution of PE PEG2000 from 50 to 25 wt % (swelling equilibrium), the spacing increases from D = 70 Å to D = 78 Å. Similarly, for PU PEG4000 the spacing increases from D = 108 Å at 25 wt % to D = 134 Å at 12.5 wt % (swelling equilibrium), and for PU PEG8000 D increases from 165 Å at 25 wt % to 175 Å at 7.5 wt % (swelling equilibrium).

For each of these polymers, the number density of the nanodomains (which is proportional to $1/D^3$) decreases more slowly than the weight fraction of polymer, indicating that the size of the domains decreases with dilution (see below for a detailed discussion).

Since the D spacing depends on the weight fraction of DFA segments in the polymer, it will depend on the PEG chain length as well. The profiles plotted in Figure 5b indeed show that q_{max} shifts to lower values as the molecular weight of PEG is increased. The correlation of peak position and spacer length indicate that the PEG spacers primarily set the characteristic D spacing (Figure 5b, inset). Similar dependency of D spacing on concentration and PEG molecular weight has been reported for other PEG based networks or gels.[45−47]

In addition, all spectra show a smooth, featureless upturn toward the lowest q scattering vectors, which is most likely due to network defects or structural heterogeneities on larger length scale. In related works on gels, thermal and frozen-in concentration fluctuations have been made responsible for this extra scattering intensity.[48] Whereas a semidilute solution of chains in a solvent is typically described by an Ornstein−Zernike model in terms of the mesh size $\zeta \sim 20$ Å typically of

DOI: 10.1021/acs.macromol.7b00319
Macromolecules 2017, 50, 3333−3346

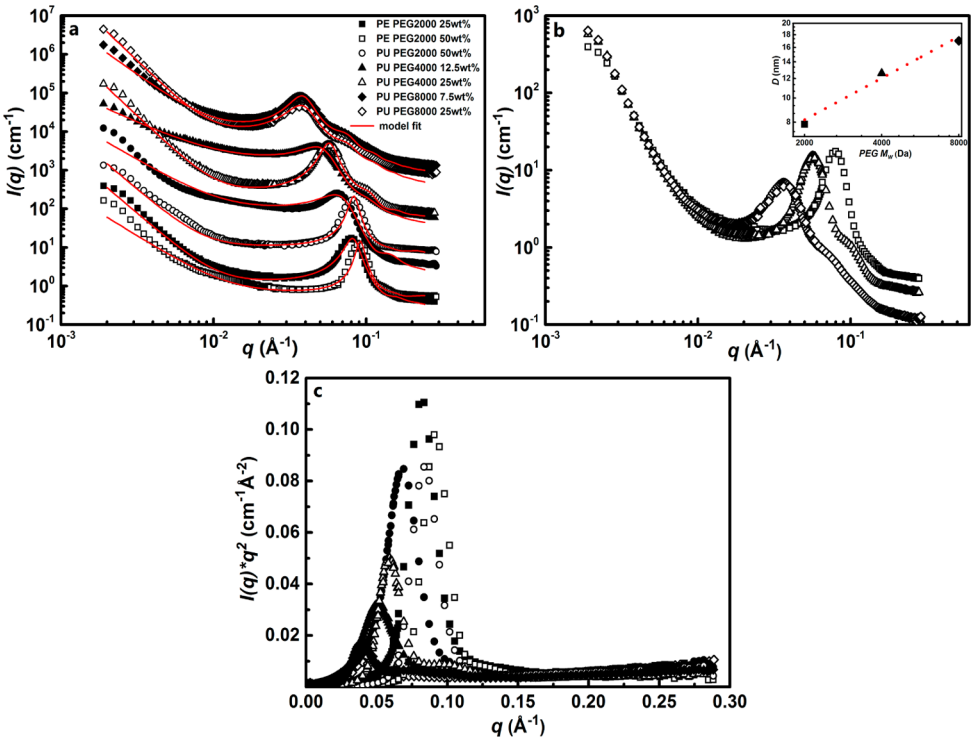

Figure 5. (a) SANS intensity profiles for hydrogel samples in D_2O at different concentrations; spectra have been shifted vertically for clarity. The symbols represent experimental data, while the red solid curves represent model fits. (b) SANS profiles of three samples with different PEG chain lengths (2K, 4K, and 8K); inset shows correlation between D and PEG molecular weight. (c) Kratky plots of all samples.

the blob network and would imply $I(q) \sim I_{OZ}/(1 + (q\zeta)^2) \sim q^{-2}$, the introduction of cross-links intrinsically leads to regions which are less accessible or fully deprived of solvent.[42] Their scattering contributions are caught by a Debye−Bueche law, $I(q) \sim I_{DB}/(1 + (q\zeta)^2)^2 \sim q^{-4}$, where now the correlation length corresponds to frozen inhomogeneities. Anticipating the evaluation, since none of these limiting power laws can be recognized and experimentally an exponent between 2 and 3 is observed, we may already conclude that both length scales are probably of the same order of magnitude. In Figure 5c we present the SANS data in so-called Kratky plots, where the interdomain peak is emphasized and parasitic scattering, corresponding to any type of inhomogeneities encountered in polymer gels, is minimized.[49]

In a study performed by Saffer et al.[47] a SANS analysis of covalently cross-linked, tetrafunctional PEG hydrogels was also examined. In several aspects the system is similar to the present, in terms of exploring the effect of different chain length of PEG on the hydrogel microstructure. However, the characteristic D spacing is only observed for the shortest PEG used (4K) at sufficiently high concentration, and it was not considered in the fitting to the correlation length model. In our hydrogels, due to a large hydrophobic moiety used, the correlation peak is present even at lower concentrations because the phase separation is much more pronounced; therefore, we were able to go further and analyze in detail the morphology of the phase-separated domains as well as the interaction distances between them.

Quantitatively, more insight into the nanostructure of the hydrogel networks can be obtained by fitting the experimental SANS data to a theoretical model. The total scattering intensity of a general three-component mixture can be written as

$$I(q) = \sum_{i,j=1}^{3} \rho_i \rho_j S_{ij}(q) \tag{2}$$

which due to incompressibility, i.e. the volume conservation hypothesis, can be rewritten as

$$I(q) = (\rho_1 - \rho_3)^2 S_{11}(q) + (\rho_2 - \rho_3)^2 S_{22}(q) + 2((\rho_1 - \rho_3)(\rho_2 - \rho_3))S_{12}(q) \tag{3}$$

where the indices 1, 2, and 3 here refer to the DFA clusters, PEG chains, and D_2O solvent, respectively.[50−52] The solvent was used as the background component and was eliminated, so only its contrast remained.

The partial structure factor $S_{ii}(q)$ is defined as $\phi_i V_i P_{ii}(q)$ for noninteracting components with volume fraction ϕ, volume of the scatterer V, and (intraparticle or intrachain) form factor $P(q)$. Interaction between the DFA clusters is included by multiplying their $P(q)$ by the hard-sphere Percus−Yevick (PY) structure factor $S_{HS}(q)$. The latter is well discussed in the literature and is not repeated here.[53−55] The cross-term $S_{ij}(q)$ which describes the correlation between DFA and PEG is considered low, not only due to the $\sqrt{\phi_1\phi_2}$ front factor that can be neglected in the present concentration range of DFA but also to the missing structural correlation between the morphology of the cluster and the PEG chains. This assumption of putting $S_{12}(q) \sim 0$ corresponds thus to dispersing unattached DFA clusters, characterized by $S_{11}(q)$, into the gel. Latter is equivalent to a small-angle X-ray (SAXS) experiment which does not distinguish between D_2O and PEG due to comparable electron densities.

To estimate the contribution of the PEG chains, given by the $S_{22}(q)$ terms, in view of the dilution degrees, we may average

DOI: 10.1021/acs.macromol.7b00319
Macromolecules 2017, 50, 3333−3346

Table 2. Fitted and Calculated Structure Parameters of PEG-DFA Hydrogels

sample	mean micellar radius R_m[a] [Å]	σ_R[a] [Å]	micellar equivalent hard-sphere radius R_{HS}[a] [Å]	micellar radius R[b] [Å]	aggregation number N_{agg}[b]
PE PEG2000 25 wt %	32.9 ± 0.3	4.6 ± 0.2	40.8 ± 0.2	35.1 ± 1.8	188 ± 30
PE PEG2000 50 wt %	26.8 ± 0.6	2.7 ± 0.5	38.7 ± 0.2	40.2 ± 3.8	283 ± 82
PU PEG2000 50 wt %	29.3 ± 0.4	2.9 ± 0.4	42.2 ± 0.2	43.7 ± 3.9	363 ± 93
PU PEG4000 12.5 wt %	56.0 ± 0.7	11.6 ± 0.3	58.3 ± 0.2	38.9 ± 4.3	258 ± 86
PU PEG4000 25 wt %	40.0 ± 0.6	7.3 ± 0.4	57.9 ± 0.2	41.5 ± 2.2	310 ± 49
PU PEG8000 7.5 wt %	63.6 ± 1.0	18.6 ± 0.5	82.2 ± 0.3	35.6 ± 2.2	196 ± 36
PU PEG8000 25 wt %	65.6 ± 1.2	19.6 ± 0.6	80.7 ± 0.2	52.5 ± 3.4	632 ± 124

[a]Percus−Yevick fit parameters to SANS data from hydrogels in D_2O at room temperature. [b]Calculated from the average intermicellar distances from the scattering profiles.

the gel phase over PEG and D_2O, yielding an average $\langle\rho_s\rangle = \phi_2\rho_2 + \phi_3\rho_3$. If ρ_3 is substituted by $\langle\rho_s\rangle$ and using $(1 - \phi_2) = \phi_1 + \phi_3$, we obtain

$$I(q) = (\rho_1 - \langle\rho_s\rangle)^2 S_{11}(q) + \phi_3(\rho_2 - \langle\rho_s\rangle)^2 S_{22}(q) \quad (4)$$

The second part of the intensity is identified with the gel scattering and $S_{22}(q)$ leads to the previously discussed extra scattering, i.e. $S_{22}(q) = S_{22}(0)/(1 + (q\zeta)^m) \sim S_{22}(0)(1 - (q\zeta)^m)$ at low q. Here, m is the generalized exponent, experimentally $2 < m < 3$. For $q\zeta = 1$ this contribution vanishes. If we set the lower bound of intensity which can be reliably detected as about 0.01 cm^{-1}, i.e., 5 times lower than the experimental incoherent scattering level of the D_2O solvent, the correlation length is of the order of ∼100 Å (∼D from the qualitative description). Assuming that in these networks spherical aggregates of DFA are formed, interacting according to a Percus−Yevick hard-sphere interaction potential, the distance between their centers of mass can be obtained from a fit to the eq 4, including $S_{HS}(q)$ in $S_{11}(q)$ and taking into account an additional incoherent background of the hydrogenous components. The solvent was subtracted before. In the evaluation of $S_{11}(q)$, we have assumed that the DFA clusters have a Gaussian distribution:

$$w(R) = \frac{1}{\sqrt{2\pi\sigma^2}} e^{(-(R-R_m)^2/2\sigma^2)} \quad (5)$$

with w being the weight and R the DFA cluster radius. R_m is the mean radius of the distribution with standard deviation σ_R.

The resulting spherical form factor $\langle P(q)\rangle$, accounted for polydispersity, is given as

$$\langle P(q, R, \sigma_R)\rangle = \frac{\int_0^\infty w(R)\left(\frac{4\pi}{3}\right)R^3\left(\frac{3(\sin(qR) - qR\cos(qR))}{(qR)^3}\right)^2 dR}{\int_0^\infty w(R)\, dR} \quad (6)$$

with

$$\langle V_p\rangle = \frac{\int_0^\infty w(R)\left(\frac{4\pi}{3}\right)R^3\, dR}{\int_0^\infty w(R)\, dR} \quad (7)$$

Although the distribution is normalized by definition, and the integration is performed numerically, the denominator corrects for eventual cutoffs. In the local monodisperse approximation, the PY structure factor is independent of the polydispersity.

In total, a description with the above form and structure factor provides values for the mean radius of the DFA micelles R_m, their distribution width σ_R, and the equivalent hard-sphere radius R_{HS}. As can be seen from Figure 5a, a reasonable agreement was found between experimental data and the model function, except for the sample PU PEG2000 at 25 wt %, which is most likely due to some larger macroscopic inhomogeneities present in the sample. However, even though the fit is not perfect, by qualitative analysis we assessed that the scattering profile, being similar to the rest of the samples, describes the same structural features. Good fits were obtained for our samples over the large q region, including the medium q range, which contains the most important information on the structure, unlike in the work of Saffer et al.[47] where the peaks were left out of consideration. The fitted parameters are shown in Table 2. Whereas we mostly relied on the q-dependence of the intensity, we further emphasize the complementary power of the calibration of scattering in absolute units. If the forward scattering intensity at $q = 0$ of the DFA cluster $S_{11}(0)$ is calculated, using the former assumption of the preaveraged solvent mixture, and from this volume the average radius $\langle R\rangle$, then an agreement with R_m within 5% is obtained. This internal consistency sustains the value of the absolute calibration as well as the used model.

Furthermore, from the average intermicellar distances, and by applying the law describing the distribution of the nearest neighbor in a random packing of particles (micelles), it was possible to estimate the number density of micelles. The following equation was employed:

$$D = 0.55396n^{-1/3} \quad (8)$$

where n is the number density of micelles.[56] Moreover, from the micellar concentration and known volume fractions of the DFA component in the samples, it was also possible to derive the volume of a single micelle of DFA and consequently its mean radius R. Finally, the aggregation number of micelles, N_{agg}, corresponding to the number of DFA units per micelle was obtained from the additivity of volumes:

$$N_{agg} = \frac{4\pi R^3 d_{DFA} N_A}{3M_{w(DFA)}} = \frac{V}{V_{DFA}} \quad (9)$$

where d_{DFA}, N_A, and $M_{W(DFA)}$ are the density of the DFA, Avogadro's number, and the molecular weight of DFA, respectively, and R is the micelle core radius calculated from the average intermicellar distance. The calculated values for micelle core radius R and aggregation number N_{agg} are listed in Table 2. From the calculated values, we observe that DFA micelles are characterized by an increase in the mean core radius R as a function of both polymer concentration and PEG molecular weight, going from 35.1 to 52.5 Å. In most of the samples the radius obtained by fitting the full q-range with the PY model is within error range (σ_R) of the radius calculated

DOI: 10.1021/acs.macromol.7b00319
Macromolecules 2017, 50, 3333−3346

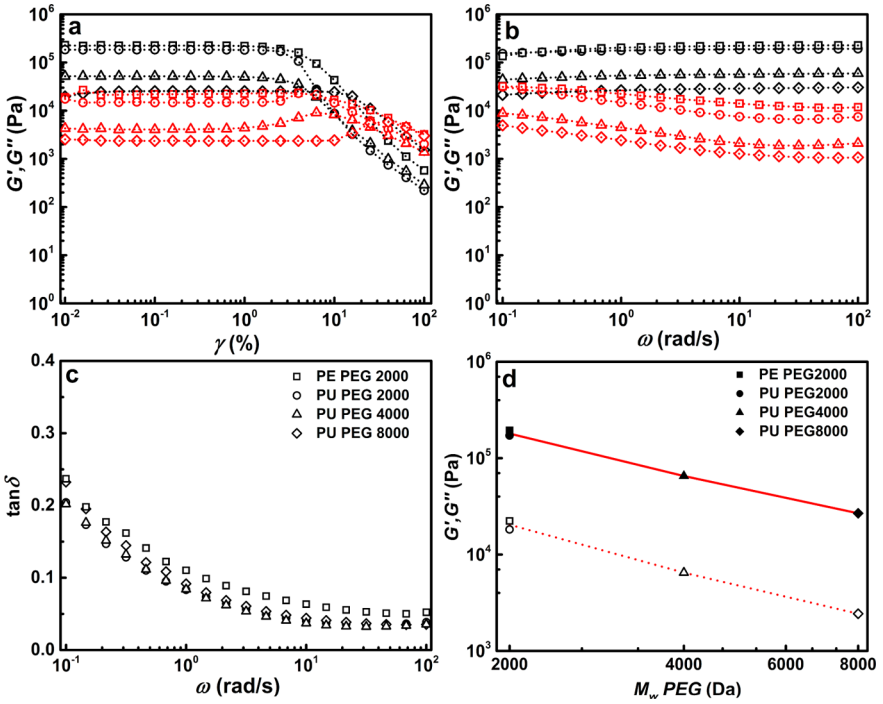

Figure 6. (a) Strain sweep at ω = 1 rad/s at 25 °C and 25 wt % concentration of all hydrogels; (b) frequency sweep at γ = 0.1% at 25 °C (■, PE PEG2000; ●, PU PEG2000; ▲, PU PEG4000; ◆, PU PEG8000; black symbols, G'; red symbols, G''); (c) loss factor tan δ as a function of angular frequency, calculated from the data in part b; (d) dependence of G' and G'' on the molecular weight of PEG (closed symbols, G'; open symbols, G'').

from the D spacing. As expected, N_{agg} show similar dependencies on the concentration and PEG molecular weight, ranging from 188 to 632.

Overall, the SANS analysis suggests that the present hydrogel networks are formed via the self-assembly of DFA units into spherical domains, representing the cross-link points. Considering that the density number of micelles is in the range of 10^{19}−10^{20} micelles/L and the average aggregation numbers are large, we can conclude that there is a strong phase separation between DFA domains and PEG swollen matrix. These results provide strong support for the network structure proposed in Figure 4.

Viscoelastic Properties of Hydrogels and Cross-Link Density. The viscoelastic properties of the PEG-DFA based hydrogels were determined via oscillatory shear rheology measurements. Figure 6a,b displays log−log plots of the shear moduli as a function of strain (γ) and angular frequency (ω), respectively. Strain sweep measurements (γ = 0.01−100%) were performed in order to determine the extension of the linear viscoelastic region for these materials. With the exception of PU PEG8000, which only starts yielding at around 15% strain, the hydrogels have moduli independent of the strain amplitude up to 4%, after which they start yielding. This is most likely due to the presence of long PEG8000 chains which contributes to increased flexibility of the system. Unless stated otherwise, in the rheological measurements, maximum strain was 0.1%, to stay within the linear viscoelastic regime. Figure 6b shows the frequency dependence of the moduli. The pattern is typical of that of chemical and other strongly interacting physical hydrogels.[29,57,58] At a concentration of 25 wt %, the storage modulus $G'(\omega)$ is frequency independent, whereas the loss modulus $G''(\omega)$ has very weak dependence in the frequency range of 0.1−100 rad/s for all hydrogels. Nonetheless, $G''(\omega)$ displayed a slight upturn toward lower frequencies, indicating a structural relaxation process and therefore a certain dynamic, nonpermanent nature of these hydrogels.[58,59] This is also evident when the loss tangent (tan $\delta = G''/G'$) is plotted against frequency, which shows an upturn of tan δ with a decrease of frequency (Figure 6c). This feature indicates an increase of viscous contributions to the material's response. However, given that for all samples G' is larger than G'', our hydrogels show predominant solid-like, elastic behavior within the range of frequencies studied. This indicates that the lifetime of the reversible cross-links in the system is longer than the slowest time scales accessed in our oscillatory rheology experiments.

The mechanical properties of the gels depend strongly on their composition, in particular on the molecular weight of PEG incorporated in the system. This dependence is shown in Figure 6d. The hydrogel with the shortest PEG segments (PEG2000) has higher values of G' and G'' than the other gels. This observation is in good agreement with the previously discussed swelling and EWC studies, which show similar trends. In fact, as the molecular weight of PEG decreases, the amount of the retained water is also lower, reflected in a lower EWC. As a consequence, the resulting hydrogel is stiffer.

The rheological measurements show that indeed G' decreases with increasing molecular weight of PEG. In general, the elastic shear modulus G' of a network depends on the density of elastically active segments and on the cross-link functionality as expressed in eq 10.[60,61]

Therefore, assuming that all DFA segments are aggregated, we estimated the modulus of each gel based on the density of PEG chains, which can be calculated directly from the degree of swelling and the composition of each segmented copolymer.

$$G = \left(1 - \frac{2}{f}\right) v_e RT v_2^{2/3} \tag{10}$$

DOI: 10.1021/acs.macromol.7b00319
Macromolecules 2017, 50, 3333−3346

Table 3. Parameters, Cross-Link Densities, and Moduli of Hydrogels at 25 °C

sample	q_f	υ_2 (volume fraction)	d_p [g/mL]	υ_e (chain density) [mol/m^3]	G' predicted [kPa]	G' measured [kPa]
PE PEG2000 25 wt %	4	0.22	1.15	98	89.1	194
PU PEG2000 25 wt %	4	0.22	1.15	98	89.1	172
PU PEG4000 25 wt %	4	0.22	1.17	54.9	49.9	55.5
PU PEG8000 25 wt %	4	0.22	1.18	29.2	26.6	26.8

where υ_e is the cross-link density due to chains, υ_2 is the volume fraction of the segmented copolymer, R is the gas constant, T is the absolute temperature, and f is the functionality of the cross-links. This is valid if we assume that the present system is a phantom network, which generally is true for the transient and nonentangled networks. Furthermore, according to the SANS analysis (Table 2), aggregation numbers are large in these hydrogels, so the cross-link functionality f is expected to be large as well. Therefore, $(1 - 2/f) \sim 1$ and virtually affine behavior is observed.[27,61] The volume fraction υ_2 was calculated by using the equation described by Gundogan:[62]

$$\upsilon_2 = \frac{1}{1 + \frac{(q_f - 1)d_p}{d_s}} \tag{11}$$

where q_f is the ratio of the weights of the swollen gel and originally dried sample, d_p is the polymer density, and d_s is the density of water (1.00 g/mL). The values of different parameters, including calculated chain densities and resulting moduli are listed in Table 3.

The predicted modulus G' for PU PEG4000 and PU PEG8000 is very close to experimentally observed values. At the same volume fraction of the polymer, the modulus of the hydrogel is inversely proportional to PEG segment molecular weight. Indeed, PU PEG4000 is twice as stiff as PU PEG8000 (49.9 kPa compared to 26.6 kPa). However, according to this observation, the modulus for PE PEG2000 and PU PEG2000 hydrogels is expected to be around 89 kPa, whereas experimentally found values are 194 and 172 kPa, respectively. Crowding of the hard spheres of the DFA micellar clusters may contribute to the higher modulus of the gel with the shortest PEG segments. These spheres have an effective radius that is increased by crowding of the PEG chains at the interface of the micelles. In the PEG2000 gels these spheres form a larger volume fraction than in the PEG4000 and the PEG8000 gels.

Transient and Reversible Nature of the Hydrogel Networks. Dynamic properties and transient character of these hydrogels were investigated with rheology measurements, in particular stress relaxation and dynamic amplitude tests. Figure 7 shows stress relaxation profiles of all four hydrogels. An initial step strain of 0.1% was applied and in all hydrogels the stress relaxation response was similar. Two regimes could be distinguished: at short times, stress decreased fast. This response at short time scales can be related to the changes occurring in the chain conformations in the network. A second regime indicated relatively slow response, but the stress had a decreasing trend even beyond the probed time scale. In this phase, structural changes were taking place. We propose that relaxation in the slow regime corresponds to a structural reorganization enabled by escape of DFA units from micelles. Since the hydrophobic segments are quite large, the interactions are very favorable, and it is expected that the disengagement of the DFA segments from the micellar cores is slow.

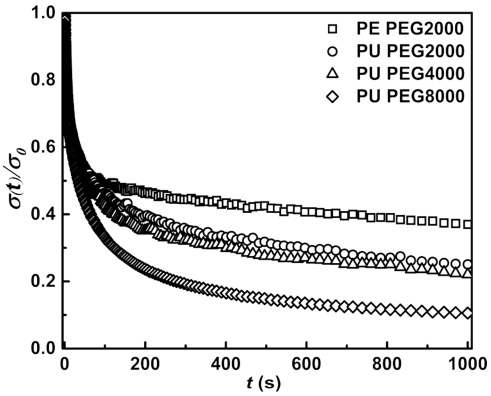

Figure 7. Stress relaxation of PEG-DFA hydrogels at 25 wt % after a step strain of 0.1%.

Stress relaxation is different for the four samples. In particular, the PU PEG8000 showed a stronger contribution of the fast component to the overall stress relaxation than the PEG2000 gels. For the former, 50% of stress was released after 30 s, whereas for the latter gel it took 76 s. After instantaneous application of strain, relaxation of the longer PEG segments in PU PEG8000 dissipate a larger fraction of the elastic energy than in the gels with shorter PEG segments. Overall, the relaxation profiles are typical of transient networks,[58,63] but here the relaxation process related to the dynamics of hydrophobic cross-links occurs at times longer than the experimental time scale of 1000 s.

In order to assess reversible character of the association present in the network, dynamic strain amplitude test was performed on PE PEG2000 hydrogel, and the response is displayed in Figure 8. The test consisted of performing alternating time and strain sweep measurements. First, time sweep was done at constant frequency (ω = 1 rad/s) and strain (γ = 0.1%), within the linear viscoelastic regime (Figure 8a). No variations in G' and G'' were observed over 600 s, indicating stable structure and consistent solid-like behavior of the hydrogel. When the sample was subjected to an increasing strain, ranging from 0.1 to 100% at 1 rad/s frequency (Figure 8b), G' and G'' were constant at small strains, but above a critical strain of 4%, G' and G'' strongly decreased. At 25% strain, a crossover point was observed, and the gel started to exhibit fluid-like character. However, when the strain was reduced back to 0.1%, the original moduli were almost immediately and fully recovered, with $G' > G''$ (Figure 8c). Thus, the gel shows yield behavior which is completely reversible (Figure 8d–g).

Temperature-Dependent Rheology. In order to investigate the effect of temperature on the viscoelastic properties of the hydrogels, a temperature sweep experiment was performed on the PE PEG2000 saturated hydrogel. Shear moduli were monitored at 1 rad/s while the temperature was varied from 25 to 75 °C. Figure 9a shows that G' decreased with temperature, whereas G'' almost remained constant, although $G' > G''$ up to

DOI: 10.1021/acs.macromol.7b00319
Macromolecules 2017, 50, 3333−3346

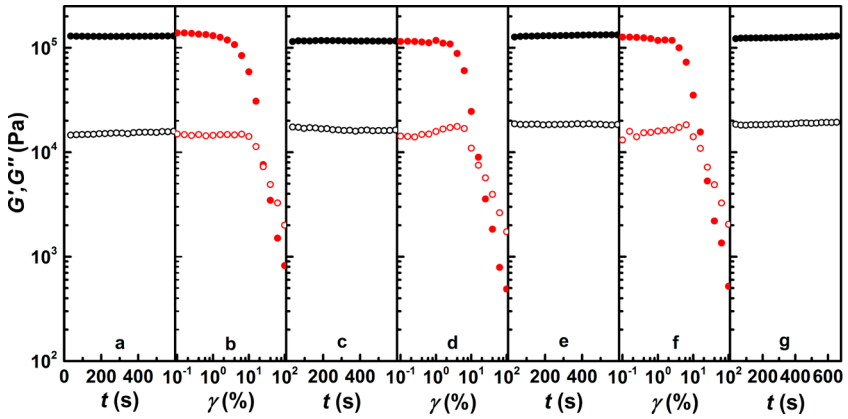

Figure 8. Dynamic strain amplitude test of PE PEG2000 at 25 °C for three alternating time sweep−strain sweep cycles (a−g).

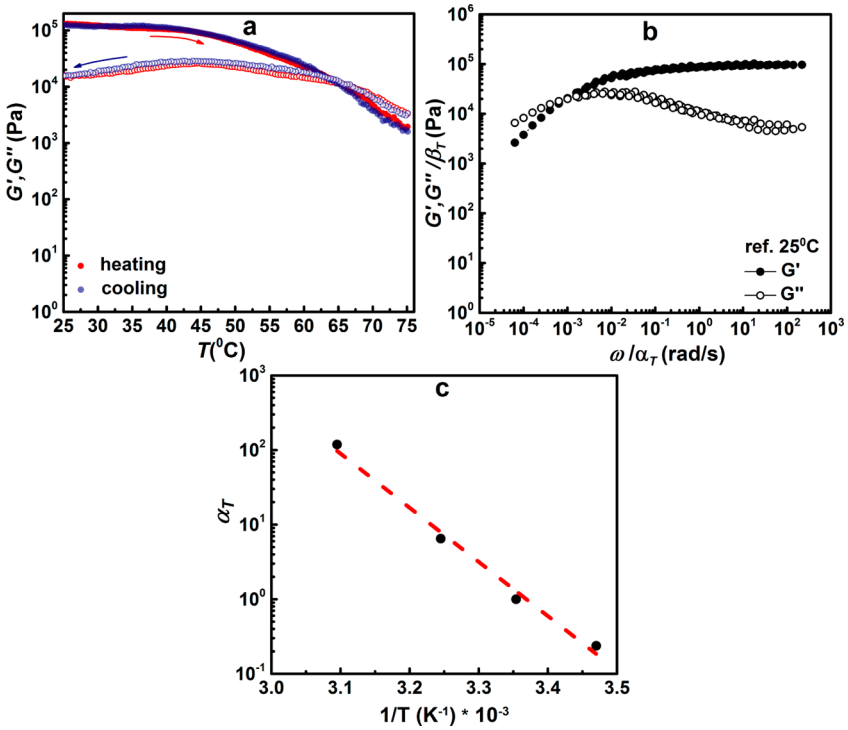

Figure 9. (a) Temperature dependence of G' (closed symbols) and G'' (open symbols) for PE PEG2000 with heating and cooling rates of 2 °C/min and at ω = 1 rad/s and γ = 0.1%. (b) Master curve obtained by time−temperature superposition, based on frequency sweeps recorded at 15, 25, 35, and 50 °C, with 25 °C taken as reference. (c) Horizontal shift factors (α_T) plotted as a function of $1/T$ (dashed red line is the exponential fit to the Arrhenius equation).

65 °C, at which temperature the gel became fluid-like. The gel to sol transition is completely reversible. Upon cooling at the same rate, both moduli increased toward higher values, as the hydrophobic association were being re-formed. At 25 °C the stiffness was fully recovered, and no hysteresis was observed during cooling. This indicates that the hydrogel presents thermoplastic properties.[64,65]

To get more insight into thermal viscoelastic behavior of these materials, frequency sweeps were performed at temperatures ranging from 25 to 65 °C, and a time−temperature superposition (TTS) master curve was constructed, which makes it possible to obtain frequency-dependent viscoelastic response over much larger frequency range. Construction of such a master curve is usually not possible for supramolecular dynamic networks, where multiple processes with different activation energies contribute to the relaxation.[66] However, for the PE PEG2000 hydrogel, a fairly decent superposition of viscoelastic responses at different temperatures was obtained, by applying both vertical and horizontal shifts (Figure 9b). The crossover point was observed at $\omega = 6 \times 10^{-4}$ rad/s. From this value, a relaxation time of 10 470 s is derived, confirming therefore long relaxation times of the present systems. This is in accordance with the previously discussed stress relaxation data.

Frequency (horizontal) shift factors (α_T), plotted against $1/T$ followed typical Arrhenius behavior (Figure 9c). The activation energy E_a for stress relaxation in the gel can be estimated to be 140 kJ/mol using eq 12.

$$\alpha_T \sim e^{\Delta E_a/RT} \tag{12}$$

It is tempting to correlate this activation energy to the activation energy for escape of a DFA unit from a micelle. In the temperature-dependent rheology studies on HEUR

DOI: 10.1021/acs.macromol.7b00319
Macromolecules 2017, 50, 3333−3346

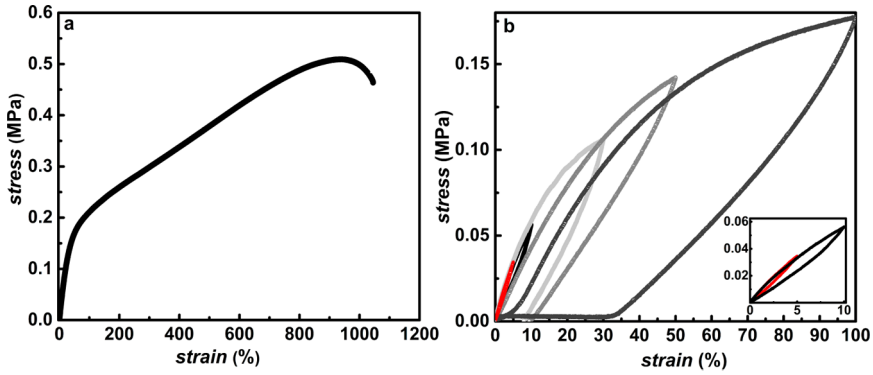

Figure 10. Tensile properties of PEG-DFA hydrogels: (a) stress−strain response of PE PEG2000; (b) recovery under cyclic loading at different maximum strains (inset plot shows more closely the behavior at 5 and 10% strain).

derivatives performed by Annable,[21] a linear relation was derived between the activation energy (E_a in kJ/mol) and the number of carbon atoms (n) present in the linear alkyl segments. The relationship was successfully applied by Kadam and co-workers in their studies on associating polymers.[67]

$$E_a = 7n - 41 \tag{13}$$

The equation predicts an activation energy of 197 kJ/mol for a DFA segment, which has 34 carbon atoms, a somewhat higher value than the value of 140 kJ/mol determined from the Arrhenius plot. Part of this difference may be related to the smaller hydrophobic surface area per carbon atom for DFA than for the linear alkanes from which the relationship was derived. It should be noted that this activation energy, while still significantly smaller than a typical sp^3-sp^3 single covalent C−C bond (~350 kJ/mol), it is close to the bond energy of weaker covalent bonds, therefore approaching the highest levels of activation energy that can be accommodated without irreversibly breaking covalent bonds.

Tensile Properties. Uniaxial tensile and cyclic loading tests were performed on equilibrium swollen PE PEG2000 (25 wt % in water), the gel which proved to be the most robust during handling. The results of tensile testing are displayed in Figure 10a as the stress−strain response, whereas derived parameters are listed in Table 4. The hydrogel displayed following results: tensile modulus E_T = 0.55 MPa, elongation at break ε_B = 1055%, tensile strength σ_T = 0.51 MPa, and tensile toughness U_T = 4.12 MJ/m^3.

Table 4. Mechanical Tensile Properties of PE PEG2000 at 25 wt %

E_T, tensile modulus (MPa)	σ_T, tensile strength (MPa)	ε_B, elongation at break (%)	U_T, tensile toughness (MJ/m^3)
0.55 ± 0.05	0.51 ± 0.05	1055 ± 42	4.12 ± 0.22

Note that the rubber-like elasticity[61] of the hydrogel is corroborated by the classical theory with $E_T = 2G(1 + \nu)$, where ν is the Poisson ratio. If we take $\nu = 1/2$ (incompressible rubbers) for the present system, we get E_T = 0.58 MPa. This is comparable to the value obtained from the stress−strain curve, suggesting a good agreement between rheology and tensile testing.

The mechanical properties are similar to those observed for other hydrogels based on segmented copolymers. In particular, the hydrogel developed by Cui et al.,[68] based on hydrophobically modified linear polyurethane−urea copolymers, exhibited similar elongation at break and toughness (ε_B = 570−1130% and U_T = 4.2−7.55 MJ/m^3). Remarkable mechanical behavior was also seen in the hydrogel system described by Meijer and co-workers.[28] Both referenced hydrogels are based on a synergistic effect of H-bonding and hydrophobic interactions. The present PEG-DFA hydrogel, however, is entirely based on hydrophobic association, which proves that if the interactions are sufficiently strong, tough hydrogels can still be obtained. The incompatibility between copolymer segments (PEG and DFA) results in phase-segregated DFA nanodomains, which act as robust physical cross-links.

The overall mechanical response and toughness of the present hydrogel were greater than those of other hydrophobically modified hydrogels,[10,69] with σ_T = 71 kPa, ε_B = 313% for polyacrylamide hydrogels modified with *N*-octylacrylamide and σ_T = 78−212 kPa, ε_B = 980−1830% for polyacrylamide hydrogels modified with octylphenol polyoxyethylene acrylate. Okay's group also showed that it was possible to make use of large hydrophobes, such as C18 and C22, which contributed to stronger hydrophobic association in the network and therefore improved toughness (σ_T = 15 kPa, ε_B = 2500%).[20] With the current polymers, high-toughness hydrogels are obtained by using even larger units (C36). Moreover, these properties are obtained without the use of micellar copolymerization preparation method to incorporate hydrophobic units, and therefore the hydrogels are stable for a longer time at the swelling equilibrium state, without dissolving or becoming more fragile.

Interestingly, PE PEG2000 hydrogel approaches some of the mechanical properties of the PAMPS/PAAm double-network (DN) hydrogel.[17] The PAMPS/PAAm DN is quite strong mechanically and is characterized by the following parameters: E_T = 0.1−1.0 MPa, σ_T = 1.0−10.0 MPa, and ε_B = 1000−2000%. This is remarkable, considering that PE PEG2000 is a single-network, supramolecular hydrogel.

These excellent mechanical properties are primarily due to DFA phase-separated domains acting as physical cross-links. In particular, the high modulus is due to a high cross-link density of PE PEG2000, as estimated previously. The DFA aggregates are multifunctional cross-linkers, as domains are composed of many DFA units. The high elongation at break is a result of the ability of DFA domains to dissipate energy. As the material is strained, DFA units dissipate energy by escaping the hydrophobic domains, yet the multifunctionality of the micelles maintains integrity of the network and keeps permanent deformation due to viscous flow. The energy dissipation

DOI: 10.1021/acs.macromol.7b00319
Macromolecules 2017, 50, 3333−3346

provides toughness because it creates resistance to crack propagation[10,58] and therefore allows elongation of the gel up to 10 times its original length.

Furthermore, cyclic loading−unloading tensile tests were performed on the same material at maximum strains between 5 and 100%, at low strain rates (0.5 mm/min). The results of these measurements are shown in Figure 10b. Interestingly, PE PEG2000 showed completely reversible, elastic behavior without permanent set at strains up to 10% (Figure 10b, inset). At larger strains the hydrogel did not completely recover its original dimensions and showed some permanent set, probably due to breakup of part of the DFA aggregates. The large hysteresis in these cyclic tests corresponds to a significant amount of dissipated energy (63 kJ/mol at 100% strain) and confirms the role of the physical cross-links in the viscoelastic properties of the gels.

CONCLUSIONS

We have developed an easy and scalable, surfactant-free preparation method for single network, tough physical hydrogels based on hydrophobic interactions. SANS measurements helped elucidate the micellar microstructure of the hydrogels, while rheology was used to establish reversible, yet long-lived cross-links. PE PEG2000 has excellent mechanical properties, including a high tensile strength (0.51 MPa), high elongation at break (1055%), toughness (4.12 MJ/m^3), and full recovery following deformations up to 10% strain. Such a high toughness is among the highest described for physical hydrogels based entirely on hydrophobic association. The high strength of the hydrophobic interactions of the DFA units in the micelles is responsible for a high activation energy for viscous flow of 140 kJ/mol. Upon straining, this results in a large dissipation of energy without breaking covalent bonds, contributing to the toughness of the material. The high functionality of the micellar cross-links limits structural changes, leading to little permanent set, even though there are no covalent cross-links.

The purely physical nature of the network in segmented PEG-DFA hydrogels offers the advantages of being easily handled, recyclable, and processable, which increases potential use of this material, in particular in applications where the heterophase structure in aqueous media could be exploited for potential controlled delivery applications of hydrophobic and amphiphilic therapeutic agents.[70]

The high modulus of PEG-DFA hydrogels, especially PE PEG2000, makes it potentially suitable for load-bearing applications in tissue engineering, such as in cartilage replacement.[71]

ASSOCIATED CONTENT

Supporting Information

The Supporting Information is available free of charge on the ACS Publications website at DOI: 10.1021/acs.macromol.7b00319.

GPC traces of the segmented copolymers, ^1H NMR spectra of the synthesized segmented copolymers (PDF)

AUTHOR INFORMATION

Corresponding Author

*E-mail R.P.Sijbesma@tue.nl.

ORCID

Marko Mihajlovic: 0000-0002-4315-0338

Notes

The authors declare no competing financial interest.

ACKNOWLEDGMENTS

This research was supported by the Marie Curie ITN project SASSYPOL (grant no. 607602, EU-FP7-PEOPLE-2013-ITN) and by the Ministry of Education, Culture and Science of The Netherlands (Gravity program 024.001.035). The small-angle neutron experiments were performed at the KWS2 instrument operated by JCNS-1 at the Heinz Maier-Leibnitz Zentrum (MLZ), Garching, Germany, and Forschungszentrum Jülich is gratefully acknowledged for providing travel support. M.M. is also thankful to Ilja Voets, Hans Heuts, and Liliana Gustini for helpful discussions.

REFERENCES

(1) Sangeetha, N. M.; Maitra, U. Supramolecular gels: Functions and uses. *Chem. Soc. Rev.* **2005**, *34*, 821−836.
(2) Van Vlierberghe, S.; Dubruel, P.; Schacht, E. Biopolymer-Based Hydrogels As Scaffolds for Tissue Engineering Applications: A Review. *Biomacromolecules* **2011**, *12*, 1387−1408.
(3) Peppas, N. A.; Hilt, J. Z.; Khademhosseini, A.; Langer, R. Hydrogels in Biology and Medicine: From Molecular Principles to Bionanotechnology. *Adv. Mater.* **2006**, *18*, 1345−1360.
(4) Drury, J. L.; Mooney, D. J. Hydrogels for tissue engineering: scaffold design variables and applications. *Biomaterials* **2003**, *24*, 4337−4351.
(5) Hoffman, A. S. Hydrogels for biomedical applications. *Adv. Drug Delivery Rev.* **2002**, *54*, 3−12.
(6) Lee, K. Y.; Mooney, D. J. Hydrogels for Tissue Engineering. *Chem. Rev.* **2001**, *101*, 1869−1880.
(7) Calvert, P. Hydrogels for Soft Machines. *Adv. Mater.* **2009**, *21*, 743−756.
(8) Bastide, J.; Leibler, L. Large-scale heterogeneities in randomly cross-linked networks. *Macromolecules* **1988**, *21*, 2647−2649.
(9) Brown, H. R. A Model of the Fracture of Double Network Gels. *Macromolecules* **2007**, *40*, 3815−3818.
(10) Abdurrahmanoglu, S.; Can, V.; Okay, O. Design of high-toughness polyacrylamide hydrogels by hydrophobic modification. *Polymer* **2009**, *50*, 5449−5455.
(11) Sakai, T.; Matsunaga, T.; Yamamoto, Y.; Ito, C.; Yoshida, R.; Suzuki, S.; Sasaki, N.; Shibayama, M.; Chung, U. Design and Fabrication of a High-Strength Hydrogel with Ideally Homogeneous Network Structure from Tetrahedron-like Macromonomers. *Macromolecules* **2008**, *41*, 5379−5384.
(12) Cui, J.; Lackey, M. A.; Madkour, A. E.; Saffer, E. M.; Griffin, D. M.; Bhatia, S. R.; Crosby, A. J.; Tew, G. N. Synthetically Simple, Highly Resilient Hydrogels. *Biomacromolecules* **2012**, *13*, 584−588.
(13) Okumura, Y.; Ito, K. The Polyrotaxane Gel: A Topological Gel by Figure-of-Eight Cross-links. *Adv. Mater.* **2001**, *13*, 485−487.
(14) Haraguchi, K.; Takehisa, T. Nanocomposite Hydrogels: A Unique Organic−Inorganic Network Structure with Extraordinary Mechanical, Optical, and Swelling/De-swelling Properties. *Adv. Mater.* **2002**, *14*, 1120−1124.
(15) Tan, Y.; Xu, K.; Wang, P.; Li, W.; Sun, S.; Dong, L. High mechanical strength and rapid response rate of poly(N-isopropyl acrylamide) hydrogel crosslinked by starch-based nanospheres. *Soft Matter* **2010**, *6*, 1467−1471.
(16) Gong, J. P.; Katsuyama, Y.; Kurokawa, T.; Osada, Y. Double-Network Hydrogels with Extremely High Mechanical Strength. *Adv. Mater.* **2003**, *15*, 1155−1158.
(17) Gong, J. P. Why are double network hydrogels so tough? *Soft Matter* **2010**, *6*, 2583−2590.
(18) Hu, X.; Vatankhah-Varnoosfaderani, M.; Zhou, J.; Li, Q.; Sheiko, S. S. Weak Hydrogen Bonding Enables Hard, Strong, Tough, and Elastic Hydrogels. *Adv. Mater.* **2015**, *27*, 6899−6905.

DOI: 10.1021/acs.macromol.7b00319
Macromolecules 2017, 50, 3333−3346

(19) Sun, J. Y.; Zhao, X.; Illeperuma, W. R. K.; Chaudhuri, O.; Oh, K. H.; Mooney, D. J.; Vlassak, J. J.; Suo, Z. Highly stretchable and tough hydrogels. *Nature* **2012**, *489*, 133−136.
(20) Tuncaboylu, D. C.; Sari, M.; Oppermann, W.; Okay, O. Tough and Self-Healing Hydrogels Formed via Hydrophobic Interactions. *Macromolecules* **2011**, *44*, 4997−5005.
(21) Annable, T.; Buscall, R.; Ettelaie, R.; Whittlestone, D. The Rheology of Solutions of Associating Polymers - Comparison of Experimental Behavior with Transient Network Theory. *J. Rheol.* **1993**, *37*, 695−726.
(22) Lundberg, D. J.; Glass, J. E.; Eley, R. R. Viscoelastic behavior among HEUR thickeners. *J. Rheol.* **1991**, *35*, 1255−1274.
(23) Yekta, A.; Xu, B.; Duhamel, J.; Adiwidjaja, H.; Winnik, M. A. Fluorescence Studies of Associating Polymers in Water: Determination of the Chain end Aggregation Number and a Model for the Association Process. *Macromolecules* **1995**, *28*, 956−966.
(24) Kaneda, I.; Koga, T.; Tanaka, F. Rheological properties of physical gel formed by hydrophobically modified urethane ethoxylate (HEUR) associative polymers in methanol−water mixtures. *Rheol. Acta* **2012**, *51*, 89−96.
(25) Xu, K.; An, H.; Lu, C.; Tan, Y.; Li, P.; Wang, P. Facile fabrication method of hydrophobic-associating cross-linking hydrogel with outstanding mechanical performance and self-healing property in the absence of surfactants. *Polymer* **2013**, *54*, 5665−5672.
(26) Miquelard-Garnier, G.; Demoures, S.; Creton, C.; Hourdet, D. Synthesis and Rheological Behavior of New Hydrophobically Modified Hydrogels with Tunable Properties. *Macromolecules* **2006**, *39*, 8128−8139.
(27) Tuncaboylu, D. C.; Sahin, M.; Argun, A.; Oppermann, W.; Okay, O. Dynamics and Large Strain Behavior of Self-Healing Hydrogels with and without Surfactants. *Macromolecules* **2012**, *45*, 1991−2000.
(28) Guo, M.; Pitet, L. M.; Wyss, H. M.; Vos, M.; Dankers, P. Y. W.; Meijer, E. W. Tough Stimuli-Responsive Supramolecular Hydrogels with Hydrogen-Bonding Network Junctions. *J. Am. Chem. Soc.* **2014**, *136*, 6969−6977.
(29) Pawar, G. M.; Koenigs, M.; Fahimi, Z.; Cox, M.; Voets, I. K.; Wyss, H. M.; Sijbesma, R. P. Injectable Hydrogels from Segmented PEG-Bisurea Copolymers. *Biomacromolecules* **2012**, *13*, 3966−3976.
(30) Peppas, N. A.; Keys, K. B.; Torres-Lugo, M.; Lowman, A. M. Poly(ethylene glycol)-containing hydrogels in drug delivery. *J. Controlled Release* **1999**, *62*, 81−87.
(31) West, J. L.; Hubbell, J. A. Comparison of covalently and physically cross-linked polyethylene glycol-based hydrogels for the prevention of postoperative adhesions in a rat model. *Biomaterials* **1995**, *16*, 1153−1156.
(32) West, J. L.; Hubbell, J. A. Polymeric Biomaterials with Degradation Sites for Proteases Involved in Cell Migration. *Macromolecules* **1999**, *32*, 241−244.
(33) Cruise, G. M.; Scharp, D. S.; Hubbell, J. A. Characterization of permeability and network structure of interfacially photopolymerized poly(ethylene glycol) diacrylate hydrogels. *Biomaterials* **1998**, *19*, 1287−1294.
(34) Breuer, T. E. In *Kirk-Othmer Encyclopedia of Chemical Technology*; John Wiley & Sons, Inc.: 2000; pp 1−13.
(35) Montarnal, D.; Cordier, P.; Soulié-Ziakovic, C.; Tournilhac, F.; Leibler, L. Synthesis of self-healing supramolecular rubbers from fatty acid derivatives, diethylene triamine, and urea. *J. Polym. Sci., Part A: Polym. Chem.* **2008**, *46*, 7925−7936.
(36) Feng, G.; Qu, H.; Cui, Y.; Li, H.; Lu, K. Synthesis and kinetic studies on dimer fatty acid/polyethylene glycol polyester. *J. Polym. Res.* **2007**, *14*, 115−119.
(37) Guelcher, S. A.; Gallagher, K. M.; Didier, J. E.; Klinedinst, D. B.; Doctor, J. S.; Goldstein, A. S.; Wilkes, G. L.; Beckman, E. J.; Hollinger, J. O. Synthesis of biocompatible segmented polyurethanes from aliphatic diisocyanates and diurea diol chain extenders. *Acta Biomater.* **2005**, *1*, 471−484.
(38) Akay, G.; Hassan-Raeisi, A.; Tuncaboylu, D. C.; Orakdogen, N.; Abdurrahmanoglu, S.; Oppermann, W.; Okay, O. Self-healing hydrogels formed in catanionic surfactant solutions. *Soft Matter* **2013**, *9*, 2254−2261.
(39) Matsen, M.; Schick, M. Stable and Unstable Phases of a Diblock Copolymer Melt. *Phys. Rev. Lett.* **1994**, *72*, 2660−2663.
(40) Bates, F. S.; Fredrickson, G. H. Block copolymers - Designer soft materials. *Phys. Today* **1999**, *52*, 32−38.
(41) Mai, Y.; Eisenberg, A. Self-assembly of block copolymers. *Chem. Soc. Rev.* **2012**, *41*, 5969−5985.
(42) Tian, J.; Seery, T. A. P.; Weiss, R. A. Physically cross-linked alkylacrylamide hydrogels: Phase behavior and microstructure. *Macromolecules* **2004**, *37*, 9994−10000.
(43) Waters, D. J.; Engberg, K.; Parke-Houben, R.; Hartmann, L.; Ta, C. N.; Toney, M. F.; Frank, C. W. Morphology of Photopolymerized End-Linked Poly(ethylene glycol) Hydrogels by Small-Angle X-ray Scattering. *Macromolecules* **2010**, *43*, 6861−6870.
(44) Lin-Gibson, S.; Jones, R. L.; Washburn, N. R.; Horkay, F. Structure-property relationships of photopolymerizable poly(ethylene glycol) dimethacrylate hydrogels. *Macromolecules* **2005**, *38*, 2897−2902.
(45) Lemmers, M.; Voets, I. K.; Cohen Stuart, M. A.; van der Gucht, J. Transient network topology of interconnected polyelectrolyte complex micelles. *Soft Matter* **2011**, *7*, 1378−1389.
(46) Pape, A. C. H.; Bastings, M. M. C.; Kieltyka, R. E.; Wyss, H. M.; Voets, I. K.; Meijer, E. W.; Dankers, P. Y. W. Mesoscale Characterization of Supramolecular Transient Networks Using SAXS and Rheology. *Int. J. Mol. Sci.* **2014**, *15*, 1096−1111.
(47) Saffer, E. M.; Lackey, M. A.; Griffin, D. M.; Kishore, S.; Tew, G. N.; Bhatia, S. R. SANS study of highly resilient poly(ethylene glycol) hydrogels. *Soft Matter* **2014**, *10*, 1905−1916.
(48) Karino, T.; Shibayama, M.; Okumura, Y.; Ito, K. SANS study on pulley effect of slide-ring gel. *Phys. B* **2006**, *385*, 807−809.
(49) Shinohara, Y.; Kayashima, K.; Okumura, Y.; Zhao, C.; Ito, K.; Amemiya, Y. Small-angle X-ray scattering study of the pulley effect of slide-ring gels. *Macromolecules* **2006**, *39*, 7386−7391.
(50) Endo, H.; Miyazaki, S.; Haraguchi, K.; Shibayama, M. Structure of Nanocomposite Hydrogel Investigated by Means of Contrast Variation Small-Angle Neutron Scattering. *Macromolecules* **2008**, *41*, 5406−5411.
(51) Miyazaki, S.; Endo, H.; Karino, T.; Haraguchi, K.; Shibayama, M. Gelation Mechanism of Poly(N-isopropylacrylamide)−Clay Nanocomposite Gels. *Macromolecules* **2007**, *40*, 4287−4295.
(52) Shibayama, M. Small-angle neutron scattering on polymer gels: phase behavior, inhomogeneities and deformation mechanisms. *Polym. J.* **2011**, *43*, 18−34.
(53) Kinning, D.; Thomas, E. Hard-Sphere Interactions Between Spherical Domains in Diblock Copolymers. *Macromolecules* **1984**, *17*, 1712−1718.
(54) Glassman, M. J.; Chan, J.; Olsen, B. D. Reinforcement of Shear Thinning Protein Hydrogels by Responsive Block Copolymer Self-Assembly. *Adv. Funct. Mater.* **2013**, *23*, 1182−1193.
(55) Baxter, R. Percus-Yevick Equation for Hard Spheres with Surface Adhesion. *J. Chem. Phys.* **1968**, *49*, 2770−2774.
(56) Chandrasekhar, S. Stochastic Problems in Physics and Astronomy. *Rev. Mod. Phys.* **1943**, *15*, 1−89.
(57) Wu, J.; Ge, Q.; Mather, P. T. PEG-POSS Multiblock Polyurethanes: Synthesis, Characterization, and Hydrogel Formation. *Macromolecules* **2010**, *43*, 7637−7649.
(58) Hao, J.; Weiss, R. A. Viscoelastic and Mechanical Behavior of Hydrophobically Modified Hydrogels. *Macromolecules* **2011**, *44*, 9390−9398.
(59) Yan, H.; Frielinghaus, H.; Nykanen, A.; Ruokolainen, J.; Saiani, A.; Miller, A. F. Thermoreversible lysozyme hydrogels: properties and an insight into the gelation pathway. *Soft Matter* **2008**, *4*, 1313−1325.
(60) Treloar, L. R. G. *The Physics of Rubber Elasticity*; Oxford University Press: New York, 1975.
(61) Mark, J. E.; Erman, B. *Rubberlike Elasticity: A Molecular Primer*; John Wiley & Sons, Inc.: New York, 1988.
(62) Gundogan, N.; Okay, O.; Oppermann, W. Swelling, elasticity and spatial inhomogeneity of poly(N,N-dimethylacrylamide) hydro-

DOI: 10.1021/acs.macromol.7b00319
Macromolecules 2017, 50, 3333−3346

gels formed at various polymer concentrations. *Macromol. Chem. Phys.* **2004**, *205*, 814−823.
(63) Meng, F.; Pritchard, R. H.; Terentjev, E. M. Stress Relaxation, Dynamics, and Plasticity of Transient Polymer Networks. *Macromolecules* **2016**, *49*, 2843−2852.
(64) Wright, E. R.; McMillan, R. A.; Cooper, A.; Apkarian, R. P.; Conticello, V. P. Thermoplastic elastomer hydrogels via self-assembly of an elastin-mimetic triblock polypeptide. *Adv. Funct. Mater.* **2002**, *12*, 149−154.
(65) Fan, Y.; Zhou, W.; Yasin, A.; Li, H.; Yang, H. Dual-responsive shape memory hydrogels with novel thermoplasticity based on a hydrophobically modified polyampholyte. *Soft Matter* **2015**, *11*, 4218−4225.
(66) Seiffert, S.; Sprakel, J. Physical chemistry of supramolecular polymer networks. *Chem. Soc. Rev.* **2012**, *41*, 909−930.
(67) Kadam, V. S.; Badiger, M. V.; Wadgaonkar, P. P.; Ducouret, G.; Hourdet, D. Synthesis and self-assembling properties of α,ω-hydroxy-poly(ethylene oxide) end-capped with 1-isocyanato-3-pentadecylcyclohexane. *Polymer* **2008**, *49*, 4635−4646.
(68) Cui, Y.; Tan, M.; Zhu, A.; Guo, M. Non-covalent interaction cooperatively induced stretchy, tough and stimuli-responsive polyurethane-urea supramolecular (PUUS) hydrogels. *J. Mater. Chem. B* **2015**, *3*, 2834−2841.
(69) Jiang, G.; Liu, C.; Liu, X.; Chen, Q.; Zhang, G.; Yang, M.; Liu, F. Network structure and compositional effects on tensile mechanical properties of hydrophobic association hydrogels with high mechanical strength. *Polymer* **2010**, *51*, 1507−1515.
(70) Yin, Y.; Yang, Y. J.; Xu, H. Hydrophobically modified hydrogels containing azoaromatic cross-links: swelling properties, degradation in vivo and application in drug delivery. *Eur. Polym. J.* **2002**, *38*, 2305−2311.
(71) Spiller, K. L.; Maher, S. A.; Lowman, A. M. Hydrogels for the repair of articular cartilage defects. *Tissue Eng., Part B* **2011**, *17*, 281−299.

DOI: 10.1021/acs.macromol.7b00319
Macromolecules 2017, 50, 3333−3346